OPEN ACCESS
Journal of Multidisciplinary Applied Natural Science Vol. 5 No. 1 (2025) https://doi.org/10.47352/jmans.2774-3047.245
Check for updates
Research Article

Optimizing Solar Power: The Impact of N719 Dye Concentration on DSSC Efficiency with TiO_2 Nanoparticles

Hardani Hardani*, Ho Soonmin, Khaerus Syahidi, Alpi Zaidah, Sulistiyana Sulistiyana, Alpiana Hidayatulloh, Ahmad Fudholi, Lily Maysari Angraini

Received : August 9, 2024	Revised : November 25, 2024	Accepted : December 11, 2024	Online : January 19, 2025

Abstract
Dye-sensitized solar cells (DSSC) are photoelectrochemical, alternative energy source devices that convert light energy into electricity. In this study, DSSC with various concentrations (0.1, 0.5, and 1.0 mM) of N719 dye have been successfully prepared using simple steps. The X-ray diffraction results of the TiO_2 film showed that it is polycrystalline with an anatase phase (tetragonal system) having a crystallite size of about 20 nm. The absorbance spectrum of the TiO_2 film and N719 dye at various concentrations was recorded by ultraviolet-visible (UV-Vis) spectrophotometer. The bandgap energy of the TiO_2 film calculated by Tauc's formula was ~3.1 eV. The DSSC prepared using the N719 dye concentration of 1 mM achieved the highest conversion efficiency (η) of 0.298 %, respectively. Subsequently, the enhancement in efficiency was ~86 % compared with the conversion efficiency of DSSC prepared with an N719 dye concentration of 0.1 and 0.5 mM.

Keywords: dye-sensitized solar cell (DSSC), efficiency, nano-particle, N719, TiO_2

1. INTRODUCTION

The world's increasing consumption of fossil fuels, resulting in pollution of the environment and global warming, has led to more interest in renewable energy sources and their technology [1]. Dye-sensitized solar cells (DSSCs) are photoelectrochemical, alternative energy source devices that convert light energy into electricity [2] [3]. DSSCs were first proposed by O'Regan and Grätzel in 1991 [4][5]. DSSCs typically consist of nanocrystalline titanium dioxide (TiO_2) photoanode film, dye molecules, redox electrolytes, and a counter electrode in a sandwich structure as shown in Figure 1 [6]. Solar radiation is absorbed by the dye resulting in the injection of holes and electrons inside the electrolyte and the TiO_2 layer, respectively [7].

Fossil fuels have a significant environmental impact, primarily through emissions of greenhouse gases (GHGs) such as carbon dioxide (CO_2), methane, and nitrous oxide [8]. Emissions from fossil fuel combustion contribute an estimated 37.4 billion tons of CO_2 in 2024, reaching a historic high [9]. These emissions are accelerating climate change, resulting in increased global temperatures and extreme weather events [10]. In addition, fossil fuel exploration and extraction activities cause land degradation, biodiversity loss, and water pollution from oil spills and the massive use of water in extraction processes such as fracking [11].

Air pollution from fossil fuel combustion, such as sulfur dioxide and fine particulates, has negative impacts on human health, including an increased risk of respiratory diseases [12]. In addition, about 44% of GHG emissions remain in the atmosphere, affecting terrestrial and marine ecosystems, while the remainder is absorbed by oceans and land, which are beginning to show a decline in their absorption capacity [13]. These challenges highlight the need for a rapid transition to renewable energy and the application of mitigation technologies such as carbon capture to reduce overall environmental impacts [14].

The injected electrons and holes move through TiO_2 and electrolyte to the electrodes and are collected in the external circuit [15]. DSSCs have attracted considerable attention in recent years because of their low cost, simple fabrication, high incident solar light-to-electricity conversion efficiency, colorful natures, and potential economic advantages [3][4].

One of the important parts of DSSCs is the dye. The Ru complexes used in DSSCS have shown quality photovoltaic characteristics which led to

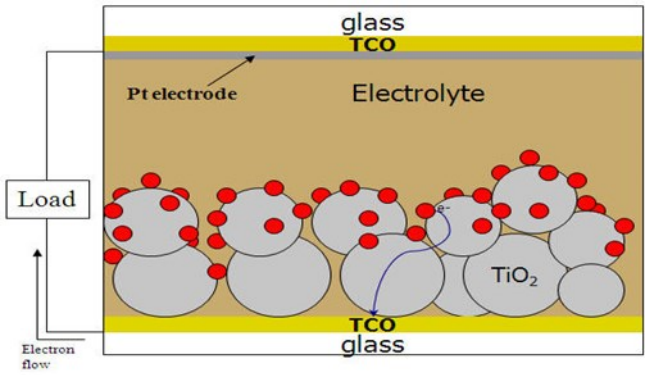

Figure 1. Dye-sensitized solar cell structure [22].

higher than 10% solar cell laboratory conditions [16][17]. The most used dye sensitizers with high photo and chemical stability are "cis-bis (isothiocyanate-bis (2,2'-bipyridy1-4,4'-dicarboxylate)ruthenium(II) bis-tetrabutylammonium" (N719). The N719 dye contains 2 carboxylic acids and 2 carboxylate groups (-COOH and COO-) whereas the carboxylate functional groups act as joining agents to immobilize the dye on the nanocrystalline TiO_2 surface [18][19]. The adsorption of N719 by the TiO_2 layer alters the electronic communication between the layer and the electrode, which is an important feature in DSSC [20][21].

This work aims to prepare a dye-sensitized solar cell by the spin-coating method and study the effect of dye concentration on solar cell efficiency. N719 dye, a ruthenium-based photosensitizer, continues to be a cornerstone in DSSCs due to its high photostability and effective light absorption across the visible spectrum [23]. Recent advancements focus on enhancing the interaction of N719 with semiconductor layers such as TiO_2 to improve electron injection and light harvesting efficiency [24]. Innovations include co-sensitization strategies where N719 is combined with organic dyes to broaden light absorption and increase energy conversion efficiency [16]. Additionally, the integration of novel redox electrolytes and advanced counter electrodes aims to mitigate electron recombination and stabilize device performance, achieving efficiencies exceeding 11% under standard illumination conditions [25]. However, challenges remain. The reliance on ruthenium makes N719 costly and raises sustainability concerns due to the metal's limited availability [26]. Furthermore, the long-term stability of N719-based DSSCs under operational conditions, such as exposure to UV light and heat, poses hurdles for commercialization [27]. Efforts to address these include exploring alternative, cost-effective organic dyes with similar or improved properties and developing encapsulation techniques to protect the dye from degradation [28]. These strategies aim to strike a balance between efficiency, cost, and scalability in DSSC technologies.

2. MATERIALS AND METHODS

2.1. Fluorine Doped Tin Oxide (FTO) Cleaning

Alcohol 70% poured on the glass of chemical as much as 100 mL. The 2.5 × 2.5 cm FTO glass to be cleaned is inserted into a glass containing chemicals. Ultrasonic cleaner was filled with distilled water to the specified limits. The chemical glass containing alcohol and FTO glass is inserted into an ultrasonic cleaner for 30 min. After that, the glass is dried using a hairdryer. Then resistance to the FTO glass using a digital multimeter [29].

FTO cleaning is performed in stages to ensure its optimal performance in applications such as DSSC [30]. The process typically starts with a wash using a detergent or mild alkaline solution, such as NaOH, to remove any oil, dust, or organic contaminants that have adhered during storage or manufacturing [31]. Then, the substrate is immersed in an alcohol or isopropanol solution to remove residual grease or water-insoluble organic contaminants [32]. This step is followed by rinsing in deionized water to avoid precipitation of ions that could affect the conductivity of the FTO [33]. Finally, the substrate is often dried in an oven or with nitrogen air to prevent stain formation or

further oxidation [34]. Each of these steps aims to ensure a clean surface, improve active film adhesion, and maintain the optoelectronic performance of the FTO.

2.2. Electrodes Preparation

The working electrode is made of FTO conductive glass on which the TiO_2 nano paste is deposited by the spin coating technique. In FTO glass measuring 2.5 × 2.5 cm formed an area for the deposition of TiO_2 measuring 2.0 × 1.5 cm above the conductive surface. The FTO side taped the tape as a barrier. The TiO_2 paste is dripped on the FTO glass that has been glued in the spinner and then stirred at a speed of 200–300 rpm with a predetermined time. The coated TiO_2 FTO glass is heated using a hotplate at 500 °C for 60 min, then cooled to room temperature [35]. The scheme of the TiO_2 paste deposition area is shown in Figure 2.

2.3. Counter Electrode Preparation

The counter electrode is an FTO conductive glass that has been coated with a thin layer of platinum (hexachloroplatinic(IV) acid 10%). The steps of making the opponent electrode are 1 mL of Hexachloroplatinic(IV) acid 10% mixed with 207 mL of isopropanol and then stirred using a vortex stirrer with a speed of 300 rpm for 30 min. The FTO glass was heated using a hotplate at 250 °C for 15 min then spilled 3 mL of the platinum solution onto the surface of the FTO glass substrate by the drop method [36]. The glass that has been dropped platinum is then cooled to reach room temperature. The scheme of the platinum deposition area is shown in Figure 3.

2.4. DSSC Sandwiching

The arrangement of DSSC layers of FTO glass that has been coated with TiO_2 and has been immersed in dye solution of extraction result is called the working electrode. The working electrode is dropped by an electrolyte solution and then covered with a platinum-coated glass called the opposing electrode. Then the DSSC arrangement is clamped with a clamp on both sides of the right and left so as not to shift [29]. The finished DSSC device is shown in Figure 4.

2.5. UV-Visible Characterization

A spectrophotometric method was used for the simultaneous determination of β-carotene [19]. The spectrophotometric method shows the potential for β-carotene analysis because pigments can absorb radiation in the visible region [37][38]. The content of each extracted material was analyzed using a Spectrophotometer UV Visible Shimadzu 1601 PC to determine the absorbance properties of the material. The wavelength range of absorption spectrum analysis in visible light is 300–800 nm. From the result of the measurement of absorbance

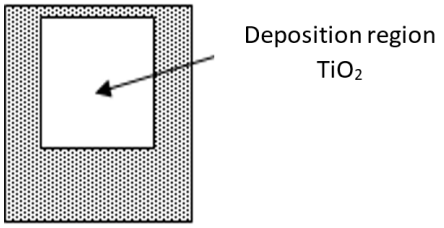

Figure 2. Schematic area of TiO_2 paste deposition.

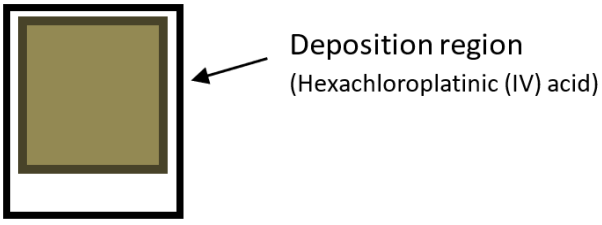

Figure 3. Platinum deposition area scheme.

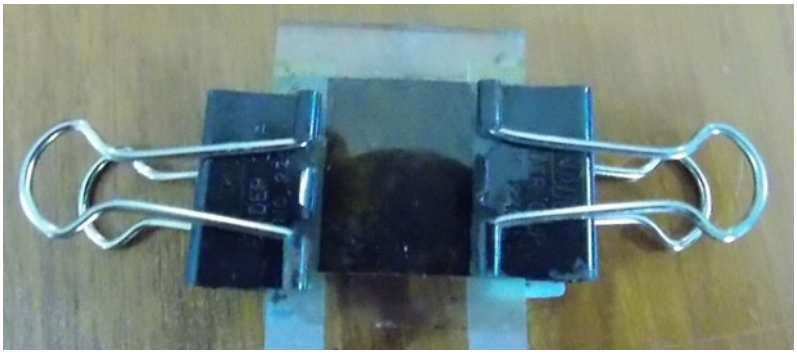

Figure 4. Results of DSSC Compilation.

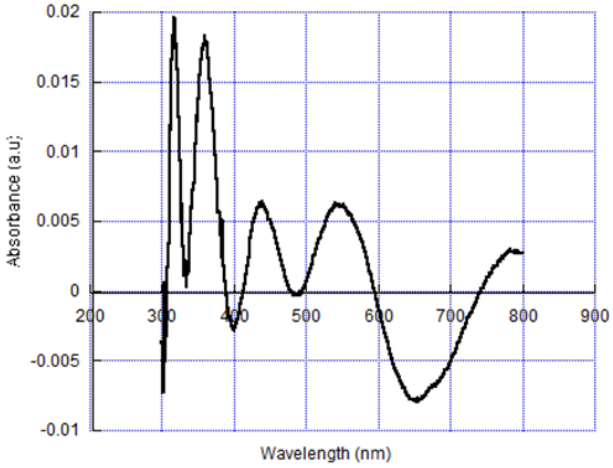

Figure 5. UV-Vis absorption spectra of concentrations 0.1% of N719 dye.

characteristics then known the type of dye content from natural material [19].

UV-Vis spectrophotometers are used to measure the absorption of light by compounds in solution, which provides information about electronic transitions and optical characteristics [39]. The wavelength range of 300–800 nm was chosen because it covers both the near UV and visible light regions, which are relevant for many optical materials, including dyes, semiconductors, and photovoltaic materials [40]. The UV region (300–400 nm) is important for detecting electronic transitions from valence electrons to higher energy levels, while the visible region (400–800 nm) measures the interaction of materials with light in the human visible spectrum [41]. The selection of this range also enables complete characterization of the absorption properties of compounds such as DSSC dyes, which often exhibit absorption peaks in this range to maximize light capture efficiency [42].

2.6. Electrical Conductivity of Material

The conductivity measurements using Elkahfi 100 / IV-Meter were performed in a dark state by covering all parts of the container using aluminum foil and under irradiation using a 100 W halogen light source and an energy intensity of 680.3 W/m^2. Halogen lamps are used because they have a full spectrum that resembles visible light with sunlight [43][44]. The result of the measurement of I-V then determined the conductivity (σ) of various materials. To determine the conductivity of the organic solution can use equation 1.

$$\sigma = 1 / \rho = l / RA \quad (1)$$

Where σ is the conductivity (ohm^{-1}.m^{-1}), R is the resistance (Ohm), l is the distance between the two electrodes (m) and A is the cross-sectional surface area of the electrode (m^2). The I-V (current-voltage) measurement setups on devices such as DSSCs are performed under highly controlled conditions to ensure accurate and reproducible data [45]. Measurements are usually performed at room temperature (around 25 °C) to reflect standard laboratory conditions and maintain device stability [46]. Lighting conditions must also be set using a solar simulator, such as a xenon or halogen lamp, calibrated at a standard light intensity of 100 mW/cm² (equivalent to 1 sun) according to the AM1.5G standard [47]. In addition, measurements were performed in an environment without ambient light (dark) to avoid interference from external light sources [48]. During the measurement, the device was placed in a fixed position with stable electrode connections to minimize fluctuations during data reading. These parameters ensure that device characteristics, such as short circuit current (Isc), open circuit voltage (Voc), fill factor (FF), and overall efficiency, can be accurately measured.

3. RESULTS AND DISCUSSIONS

3.1. Optical Properties

Figure 5 demonstrates the UV–Vis absorption spectra of the N719 dye solution with concentrations of 0.1 mM in the wavelength range of (300–800) nm. From Figure 5, it can be observed

that the increase in dye concentration leads to an increase in absorbance. Moreover, the UV-Vis absorption spectra show that the N719 dye has four absorption peaks at ~320 and 560 nm.

The UV-Vis absorption spectrum of the N719 dye solution with a concentration of 0.1 mM shows typical characteristics, where the absorbance increases as the concentration increases. This is consistent with the Beer-Lambert law, which states that the absorbance is directly proportional to the concentration of the solution and the path length of the light. Four absorption peaks at around 320 and 560 nm describe specific electronic transitions in the N719 molecule. The peak at 320 nm can be attributed to the π-π* transition in the conjugated organic ligand, while the peak in the 560 nm region is related to metal-ligand charge transfer (MLCT, metal-to-ligand charge transfer) from the ruthenium metal center to the conjugated ligand, which is a key feature in the performance of this dye as a photosensitizer [49]. These spectra also show that N719 is designed to effectively absorb light in the visible region, with significant absorption peaks in the wavelength region relevant to solar energy absorption [50]. The increase in absorbance with concentration indicates that the interaction between the dye and light becomes more efficient, which may increase the number of light-induced electrons in the DSSC device.

Figure 6 illustrates the UV-Vis absorption spectra of N719 dye solutions with a concentration of 0.5 mM across the 300–800 nm wavelength range. As the dye concentration increases, the absorbance also rises, which aligns with the Beer-Lambert law, confirming that higher concentrations result in greater absorption due to the increased number of dye molecules interacting with light. The N719 dye exhibits four distinct absorption peaks, notably around 320 and 560 nm. The peak at approximately 320 nm is attributed to the π-π* transitions in the conjugated organic ligands, while the peak around 560 nm corresponds to MLCT transition, a key feature that facilitates efficient electron injection in DSSCs. This finding corroborates research by Saehana et al. [51], which also reported that N719's absorption spans the 250–650 nm range, emphasizing the dye's broad light absorption capability in both the UV and visible regions. The absorption characteristics at these wavelengths are crucial for maximizing light harvesting efficiency, as they allow the dye to effectively absorb a significant portion of the solar spectrum. The increase in absorbance with concentration further suggests that optimizing the dye loading could enhance electron generation in DSSCs, improving overall performance.

Figure 7 shows the UV-Vis absorption spectra of the N719 dye solution at a concentration of 1 mM in the 300–800 nm wavelength range. As observed, the absorbance increases with dye concentration, which is consistent with the Beer-Lambert law, where higher concentrations lead to greater light absorption due to the increased number of dye molecules. The spectra reveal two significant absorption peaks at approximately 320 and 560 nm. The peak at around 320 nm corresponds to the π-π* electronic transitions of the organic ligands in N719, while the peak at approximately 560 nm is

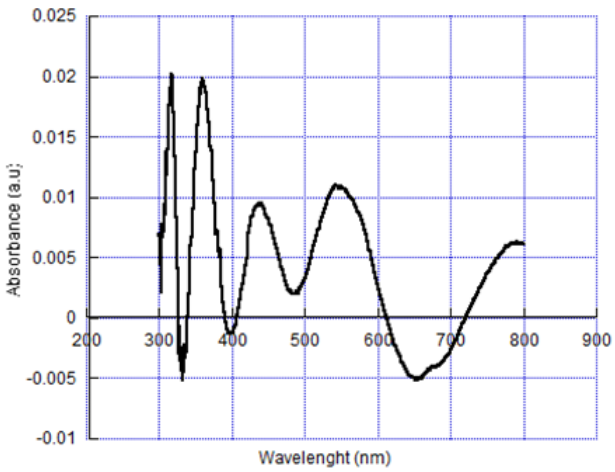

Figure 6. UV-Vis absorption spectra of concentrations 0.5% of N719 dye.

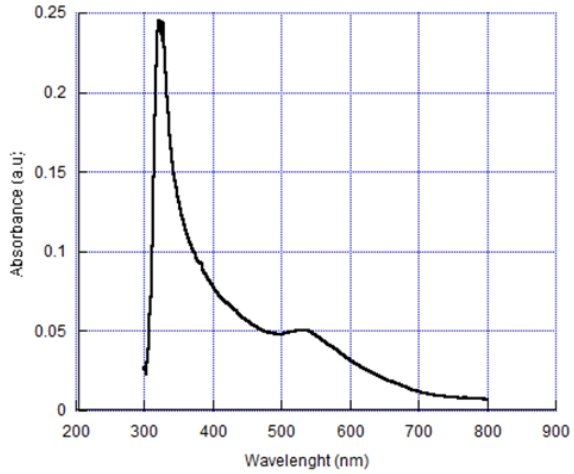

Figure 7. UV-Vis absorption spectra of concentrations 1% of N719 dye.

associated with MLCT, a critical process for efficient electron injection in DSSCs. These findings align with research by Wu, which demonstrated that DSSCs using N719 (a ruthenium-based complex dye) and other dyes like the black dye show similar absorption characteristics [52]. The broad absorption at these wavelengths allows N719 to effectively capture light across a significant portion of the solar spectrum, enhancing the efficiency of DSSCs by promoting better electron generation from absorbed photons.

3.2. Current-voltage Characteristics

Figure 8 shows the I-V characteristics of DSSC prepared by TiO_2 film thickness of 10µm annealed at 550 °C for 30 minutes and various concentrations of N719 dye (0.1, 0.5, and 1.0 mM). From the I-V curves, it was noted that "short–circuit current density" increases as the dye concentration increases. This result agrees well with the UV-Vis results (Figure 5). This result suggests that as the dye concentration increases, the TiO_2 layer adsorbs enough dye and achieves higher efficiency. The DSSC with 1 mM dye concentration has high VOC and JSC and subsequently obtained the highest efficiency. However, at low dye concentration (0.1 mM), the adsorption is low and the VOC and JSC efficiency become lower. It can be also observed that VOC changes with concentration variation which is thought to be due to the reactivity and instability of N719 [3]. This study is in line with research conducted by Zdyb and Krawzak [53], stating that the impact of various immersion times in the N719 dye solution of TiO_2-coated photoelectrodes has been investigated. In the study, the process of encapsulating the cell with a gasket sealant was improved which led to an increase in the stability and firmness of the obtained DSSC devices.

Table 1 shows the photovoltaic parameters of the DSSCs prepared using different. Concentrations of N719 dye solution and intensity. The maximum efficiency (η) of 0.298 % was achieved at a dye concentration of 1 mM and the maximum efficiency enhancement was about 86%.

The I-V (current-voltage) characteristics of dye-sensitized solar cells (DSSCs) prepared using various concentrations of N719 dye are typically analyzed to understand the impact of dye loading on cell performance. Figures 8 (a), (b), and (c) show the I-V (current-voltage) characteristics of the DSSC (dye-sensitized solar cell) under two conditions namely Bright Current and Dark Current. The bright current curve shows the response of the DSSC when exposed to light (lights on) while the dark current curve shows the leakage current or current caused by recombination of electrons in the DSSC when no light is applied. From Figure 8, the DSSC has a noticeable difference between bright current and dark current, which shows a good performance in generating current from light. However, the dark current shows a recombination rate that still needs to be minimized to improve the overall efficiency. The photovoltaic parameters of DSSCs made using various concentrations of N719 dye solution are presented in Table 1.

Table 1 presents the photovoltaic parameters of

DSSCs fabricated with varying concentrations of N719 dye solution and light intensity, with a η of 0.298% observed at a dye concentration of 1 mM. The maximum efficiency enhancement of about 86% indicates a significant improvement in device performance with increased dye concentration. This suggests that the higher dye concentration leads to a more effective light absorption, as more dye molecules are available to capture photons, thereby generating more electrons for the photovoltaic process. However, while higher concentrations can enhance absorbance and electron generation, there may be a point where excess dye causes aggregation or inefficient charge transfer, which could negatively impact performance. The improvement in efficiency is likely due to the optimized balance between dye loading and the ability of the dye to facilitate electron injection into the TiO_2 electrode. This result is consistent with previous studies showing that optimizing the dye concentration enhances the overall light harvesting and conversion efficiency in DSSCs.

Limitations in this study, especially regarding DSSCs, include aspects of stability and scalability. The stability of DSSC devices is often a challenge due to the use of liquid electrolytes that are prone to leakage, evaporation, or chemical degradation, which reduces the lifespan of the device. In addition, dyes such as N719 may undergo photodegradation under long-term exposure to UV light, resulting in decreased efficiency. Potential solutions, such as the development of solid-state electrolytes or more stable organic dyes, still face technical challenges in achieving comparable performance to conventional technologies. In terms of scalability, DSSC fabrication processes are often complex and require expensive materials, such as ruthenium in N719, which may hinder widespread commercial adoption. Further research is needed to develop efficient mass-production methods and use more sustainable materials without compromising performance.

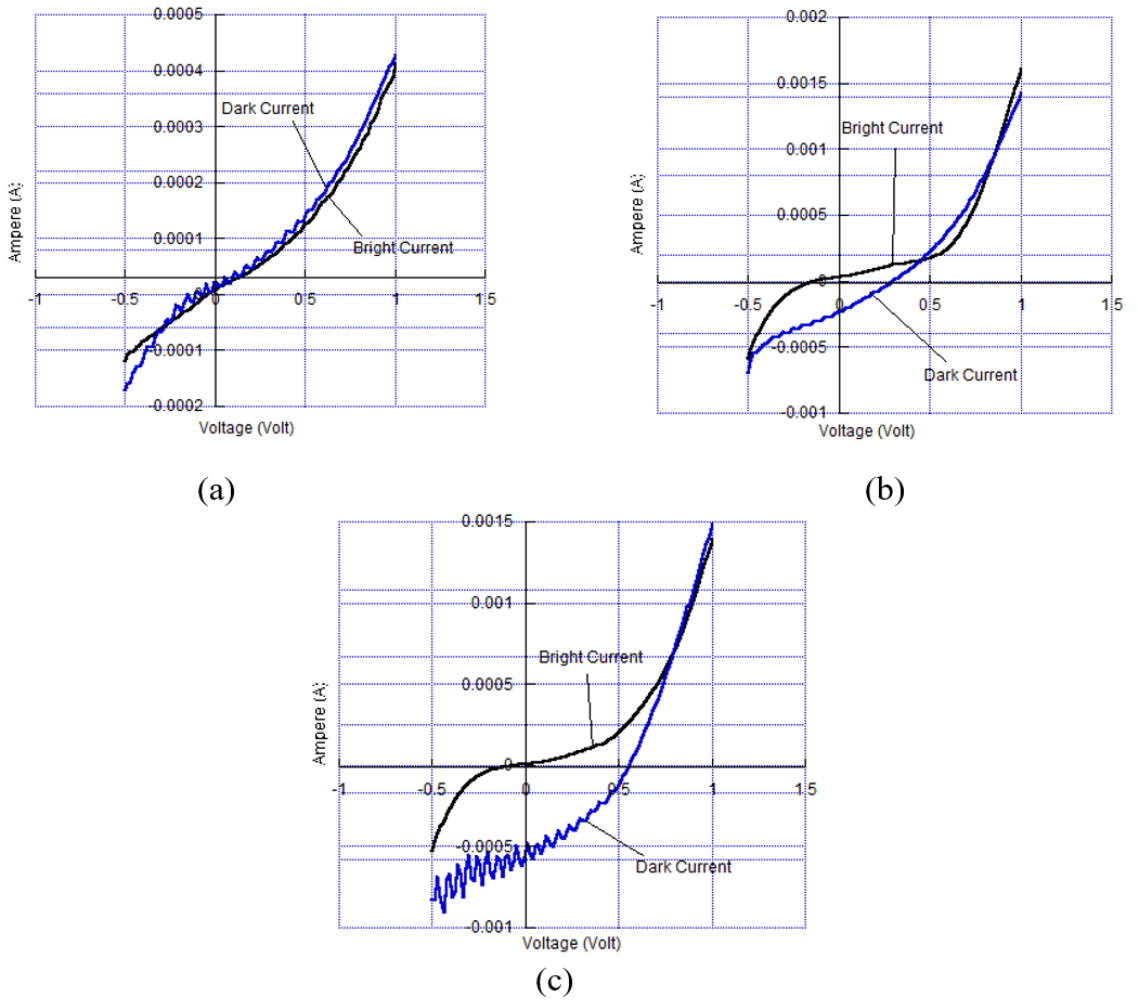

Figure 8. I-V characteristics of DSSC prepared by various concentrations of N719 dye.

Table 1. The photovoltaic parameters of DSSCs were fabricated using different concentrations of N719 dye solution.

N719 dye concentration (mM)	Intensity	Imax (Ampere)	Vmax (Volt)	Isc (Ampere)	Voc (Volt)	Fill Factor	Efficiency (%)
0.1	100	5.4×10^{-5}	0.170	9.5×10^{-6}	0.46	1.9×10^{-10}	0.024
	250	6.0×10^{-5}	0.144	9.0×10^{-5}	0.28	3.1×10^{-9}	0.035
	500	1.8×10^{-4}	0.280	3.6×10^{-4}	0.49	3.8×10^{-8}	0.103
	750	1.7×10^{-4}	0.23	3.0×10^{-4}	0.49	2.5×10^{-8}	0.055
	1000	$\mathbf{4.5\times10^{-4}}$	**0.37**	$\mathbf{7.8\times10^{-4}}$	**0.58**	$\mathbf{2.3\times10^{-7}}$	**0.169**
0.5	100	6.8×10^{-5}	0.14	3.7×10^{-5}	0.28	1.3×10^{-9}	0.018
	250	9.7×10^{-5}	0.05	1.0×10^{-4}	0.13	4.4×10^{-9}	0.021
	500	$\mathbf{2.4\times10^{-4}}$	**0.20**	$\mathbf{4.2\times10^{-4}}$	**0.34**	$\mathbf{6.2\times10^{-8}}$	**0.098**
	750	1.6×10^{-4}	0.23	2.9×10^{-4}	0.46	2.4×10^{-8}	0.052
	1000	8.4×10^{-5}	0.32	1.6×10^{-4}	0.58	7.8×10^{-9}	0.027
1.0	100	3.3×10^{-5}	0.17	5.7×10^{-5}	0.35	9.3×10^{-10}	0.058
	250	2.1×10^{-4}	0.32	4.0×10^{-4}	0.40	6.9×10^{-8}	0.273
	500	$\mathbf{5.6\times10^{-4}}$	**0.26**	$\mathbf{7.5\times10^{-4}}$	**0.46**	$\mathbf{2.4\times10^{-7}}$	**0.298**
	750	3.0×10^{-4}	0.28	5.3×10^{-4}	0.55	8.3×10^{-8}	0.112
	1000	5.2×10^{-4}	0.32	1.0×10^{-3}	0.61	2.8×10^{-7}	0.169

4. CONCLUSIONS

In this study, DSSCs with various concentrations (0.1, 0.5, and 1.0 mM) of N719 dye has been successfully prepared using simple steps. The absorbance in the The wavelength range of (300–800) nm shows that N719 dye with 1 mM concentration has The highest absorption. The DSSC prepared with 1 mM demonstrated the highest efficiency of 0.298 %. This study shows that the concentration of N719 dye has a significant effect on the efficiency of TiO_2 nanoparticle-based DSSCs. Optimal dye concentration results in maximum light absorption and efficient electron injection, while too low or too high concentration reduces performance due to lack of absorption or dye aggregation. TiO_2 nanoparticles play an important role in supporting electron transfer through a semiconductor structure with a high surface area. This dye concentration optimization emphasizes the potential of DSSCs as an efficient and environmentally friendly renewable energy solution.

AUTHOR INFORMATION

Corresponding Author

Hardani Hardani — Department of Pharmacy, Politeknik Media Farma Husada Mataram, Mataram-83122 (Indonesia);
orcid.org/0000-0003-3779-015X
Email: danylastchild07@gmail.com

Authors

Ho Soonmin — Faculty of Health and Life Sciences, INTI International University, Putra Nilai-71800 (Malaysia);
orcid.org/0000-0002-3697-5091

Khaerus Syahidi — Department of Physics Education, Universitas Hamzanwadi, Selong-83611 (Indonesia);
orcid.org/0009-0003-7059-9434

Alpi Zaidah — Department of Natural Science Education, Institut Pendidikan Nusantara Global, Praya-85311 (Indonesia);
orcid.org/0009-0003-8201-371X

Sulistiyana Sulistiyana — Department of Chemsitry, Universitas Islam Negeri Mataram, NTB-83116 (Indonesia);
orcid.org/0000-0001-7702-4869

Alpiana Hidayatulloh — Faculty of Science, Engineering and Applied Sciences, Universitas Pendidikan Mandalika, Mataram-83125 (Indonesia);
orcid.org/0009-0004-8695-7627

Ahmad Fudholi — Solar Energy Research Institute, Universiti Kebangsaan Malaysia, Selangor-43600 (Malaysia); Center for Energy Conversion and Conservation, National Research and Innovation Agency (BRIN), Jakarta-10340, (Indonesia);
orcid.org/0000-0002-9528-7344

Lily Maysari Angraini — Department of Physics, University of Mataram, Mataram-83116, (Indonesia); International Graduate Program of Molecular Science Technology, National Taiwan University, Taipei-10617 (Taiwan);
orcid.org/0000-0001-7047-8745

Author Contributions

H. H., conceptualization, methodology, investigation, validation, writing original draft; H. S., resources, and investigation; K. S., A. Z., S. S., methodology, and supervision; H. H., H. S., A. F., L. M. A., A. Z., S. S., A. H., methodology, writing, review, and editing; H. S., K. S., A. Z., A. H., S. S. supervision, conceptualization, project administration, and funding acquisition. All authors read and approved the final version of the manuscript.

Conflicts of Interest

All authors declare that there are not any conflicts of interest.

REFERENCES

[1] K. Guo, M. Li, X. Fang, X. Liu, B. Sebo, Y. Zhu, Z. Hu, and X. Zhao. (2013). "Preparation and enhanced properties of dye-sensitized solar cells by surface plasmon resonance of Ag nanoparticles in nanocomposite photoanode". *Journal of Power Sources.* **230**: 155-160. 10.1016/j.jpowsour.2012.12.079.

[2] F. H. Alharbi and S. Kais. (2015). "Theoretical limits of photovoltaics

efficiency and possible improvements by intuitive approaches learned from photosynthesis and quantum coherence". *Renewable and Sustainable Energy Reviews.* **43**: 1073-1089. 10.1016/j.rser.2014.11.101.

[3] M. Y. A. Rahman, A. A. Umar, L. Roza, and M. M. Salleh. (2014). "Effect of organic dye on the performance of dye-sensitized solar cell utilizing TiO2 nanostructure films synthesized via CTAB-assisted liquid phase deposition technique". *Russian Journal of Electrochemistry.* **50** (11): 1072-1076. 10.1134/s1023193514080114.

[4] M. Grätzel. (2005). "Photovoltaic performance and long-term stability of dye-sensitized mesoscopic solar cells". *Comptes Rendus Chimie.* **9** (5-6): 578-583. 10.1016/j.crci.2005.06.037.

[5] H. Hardani, H. Darmaja, M. I. Darmawan, C. Cari, and A. Supriyanto. (2016). "Pengaruh Perubahan Intensitas Cahaya Halogen Ruthenium (N719) Fotosensitizer Dalam Dye -Sensitized Solar Cell(Dssc)". *Jurnal Penelitian Fisika dan Aplikasinya (JPFA).* **6** (2). 10.26740/jpfa.v6n2.p70-76.

[6] Y.-F. Wang, K.-N. Li, W.-Q. Wu, Y.-F. Xu, H.-Y. Chen, C.-Y. Su, and D.-B. Kuang. (2013). "Fabrication of a double layered photoanode consisting of SnO2 nanofibers and nanoparticles for efficient dye-sensitized solar cells". *RSC Advances.* **3** (33). 10.1039/c3ra41839a.

[7] H. Soonmin, Hardani, P. Nandi, B. S. Mwankemwa, T. D. Malevu, and M. I. Malik. (2023). "Overview on Different Types of Solar Cells: An Update". *Applied Sciences.* **13** (4). 10.3390/app13042051.

[8] A. B. Omotoso and A. O. Omotayo. (2023). "The interplay between agriculture, greenhouse gases, and climate change in Sub-Saharan Africa". *Regional Environmental Change.* **24** (1). 10.1007/s10113-023-02159-3.

[9] M. Khaleel, Z. Yusupov, N. Alderoubi, R. L. Abdul_jabbar, M. Elmnifi, Y. Nassar, H. S. Majdi, L. J. Habeeb, and S. Abulifa. (2024). "Evolution of Emissions: The Role of Clean Energy in Sustainable Development". *Challenges in Sustainability.* **12** (2): 122-135. 10.56578/cis120203.

[10] S. I. Seneviratne, X. Zhang, M. Adnan, W. Badi, C. Dereczynski, A. D. Luca, S. Ghosh, I. Iskandar, J. Kossin, S. Lewis, F. Otto, I. Pinto, M. Satoh, S. M. Vicente-Serrano, M. Wehner, B. Zhou, and R. Allan. (2023). In: "Climate Change 2021 – The Physical Science Basis, ch. 11". 1513-1766. 10.1017/9781009157896.013.

[11] N. Butt, H. L. Beyer, J. R. Bennett, D. Biggs, R. Maggini, M. Mills, A. R. Renwick, L. M. Seabrook, and H. P. Possingham. (2013). "Conservation. Biodiversity risks from fossil fuel extraction". *Science.* **342** (6157): 425-6. 10.1126/science.1237261.

[12] I. Manisalidis, E. Stavropoulou, A. Stavropoulos, and E. Bezirtzoglou. (2020). "Environmental and Health Impacts of Air Pollution: A Review". *Frontiers in Public Health.* **8**: 14. 10.3389/fpubh.2020.00014.

[13] R. Hood. (2005). In: "A Companion to Applied Ethics". 674-684. 10.1002/9780470996621.ch50.

[14] A. I.Hassan and H. M.Saleh. (2024). "The challenges of sustainable energy transition: A focus on renewable energy". *Applied Chemical Engineering.* **7** (2). 10.59429/ace.v7i2.2084.

[15] C.-Y. Cai, S.-K. Tseng, M. Kuo, K.-Y. Andrew Lin, H. Yang, and R.-H. Lee. (2015). "Photovoltaic performance of a N719 dye based dye-sensitized solar cell with transparent macroporous anti-ultraviolet photonic crystal coatings". *RSC Advances.* **5** (124): 102803-102810. 10.1039/c5ra21194h.

[16] K. Sharma, V. Sharma, and S. S. Sharma. (2018). "Dye-Sensitized Solar Cells: Fundamentals and Current Status". *Nanoscale Research Letters.* **13** (1): 381. 10.1186/s11671-018-2760-6.

[17] N. A. Bakr, A. K. Ali, A. K. Ali, S. M. Jassim, and K. I. Hasoon. (2017). "Effect of N719 dye concentration on the Conversion Efficiency of Dye-Sensitized Solar Cells (DSSCs)". *Zanco Journal of Pure and Applied Sciences.* **29** (s4). 10.21271/ZJPAS.29.s4.31.

[18] J. Zhang, N. Vlachopoulos, M. Jouini, M. B. Johansson, X. Zhang, M. K. Nazeeruddin, G. Boschloo, E. M. J. Johansson, and A. Hagfeldt. (2016). "Efficient solid-state dye-sensitized solar cells: The influence of dye molecular structures for the in-situ photoelectrochemically polymerized PEDOT as hole transporting material". *Nano Energy.* **19**: 455-470. 10.1016/j.nanoen.2015.09.010.

[19] Hardani, Cari, and A. Supriyanto. (2018). "Efficiency of dye-sensitized solar cell (DSSC) improvement as a light party TiO2-nano particle with extract pigment mangosteen peel (Garcinia mangostana)". 10.1063/1.5054406.

[20] F. Li, Y. Chen, X. Zong, W. Qiao, H. Fan, M. Liang, and S. Xue. (2016). "New benzothiadiazole-based dyes incorporating dithieno[3,2-b:2′,3′-d]pyrrole (DTP) π-linker for dye-sensitized solar cells with different electrolytes". *Journal of Power Sources.* **332**: 345-354. 10.1016/j.jpowsour.2016.09.141.

[21] M. Aliofkhazraei.(2015)." Handbook of Nanoparticles. 10.1007/978-3-319-13188-7.

[22] D. Wei. (2010). "Dye-sensitized solar cells". *International Journal of Molecular Sciences.* **11** (3): 1103-13. 10.3390/ijms11031103.

[23] R. A. Afre, K. Y. Ryu, W. S. Shin, and D. Pugliese. (2024). "Comparative Study of Quasi-Solid-State Dye-Sensitized Solar Cells Using Z907, N719, Photoactive Phenothiazine Dyes and PVDF-HFP Gel Polymer Electrolytes with Different Molecular Weights". *Photonics.* **11** (8). 10.3390/photonics11080760.

[24] A. K. N. M. Yusuf, S. Mustafar, M. L. Borines, E. N. Kusumawati, and N. Hashim. (2021). "Versatility of Photosensitizers in Dye-Sensitized Solar Cells (DSSCs)". *Biointerface Research in Applied Chemistry.* **12** (6): 8543-8560. 10.33263/briac126.85438560.

[25] H. Tian and L. Sun. (2011). "Iodine-free redox couples for dye-sensitized solar cells". *Journal of Materials Chemistry.* **21** (29). 10.1039/c1jm10598a.

[26] M. R. Karim, M. A. Shar, and S. Abdullah. (2019). "Mixed Dyes for Dye-sensitized Solar Cells Applications". *Current Nanoscience.* **>15** (5): 501-505. 10.2174/1573413715666190325165613.

[27] S. N. Tamilselvan and S. Shanmugan. (2024). "Towards sustainable solar cells: unveiling the latest developments in bio-nano materials for enhanced DSSC efficiency". *Clean Energy.* **8** (3): 238-257. 10.1093/ce/zkae031.

[28] P. O. Oladoye, M. Kadhom, I. Khan, K. H. Hama Aziz, and Y. A. Alli. (2024). "Advancements in adsorption and photodegradation technologies for Rhodamine B dye wastewater treatment: fundamentals, applications, and future directions". *Green Chemical Engineering.* **5** (4): 440-460. 10.1016/j.gce.2023.12.004.

[29] H. Hardani, M. R. Harahap, and A. Suhada. (2022). "Ruthenium (N719) Optimization to Improve Dye-Sensitized Solar Cell Efficiency". *International Journal of Thin Film Science and Technology.* **11** (1): 47-53. 10.18576/ijtfst/110106.

[30] M. H. Tang, P. Chakthranont, and T. F. Jaramillo. (2017). "Top-down fabrication of fluorine-doped tin oxide nanopillar substrates for solar water splitting". *RSC Advances.* **7** (45): 28350-28357. 10.1039/c7ra02937c.

[31] S. Saehana, A. Izzah, A. J. Palamba, D. Darsikin, and N. F. A. Rahman. (2023). "Fabrication of Fluorine-Doped Tin Oxide (FTO): From experiment to its application in physics learning". *Momentum: Physics Education Journal.* **7** (2): 259-268. 10.21067/mpej.v7i2.8438.

[32] A. C. Klemz, S. E. Weschenfelder, S. Lima de Carvalho Neto, M. S. Pascoal Damas, J. C. Toledo Viviani, L. P. Mazur, B. A. Marinho, L. d. S. Pereira, A. da Silva, J. A. Borges Valle, A. A. U. de Souza, and S. M. A. Guelli U. de Souza. (2021). "Oilfield produced water treatment by liquid-liquid extraction: A review". *Journal of Petroleum Science and Engineering.* **199**. 10.1016/j.petrol.2020.108282.

[33] J. Wang, Z. Pang, F. Jin, and M. Ge. (2021). "Precipitation method to prepare conductive F-doped SnO2-coated rutile TiO2 whisker and its application in coating". *Journal of Materials Science: Materials in Electronics.*

32 (15): 20583-20597. 10.1007/s10854-021-06569-z.

[34] J. Ye, X. Zhang, S. Yuan, Y. Zhang, J. Cao, W. Teng, and Y. Wang. (2024). "An Investigation of Volatile Flavor Compounds and Lipolysis-Oxidation in Coppa as Affected by the Inoculation of Coagulase-Negative Staphylococcus during the Air-Drying Stage". *Foods.* **13** (17). 10.3390/foods13172723.

[35] H. Hardani, H. Hendra, M. I. Darmawan, C. Cari, and A. Supriyanto. (2017). "Fabrication of dye natural as a photosensitizer in dye-sensitized solar cells (DSSC)". *Journal of Physics: Theories and Applications.* **1** (1). 10.20961/jphystheor-appl.v1i1.4704.

[36] H. Hardani, A. Hidayatulloh, and L. M. A. (2018). "The Efficiency Of Dye-Sensitized Solar Cell (Dssc) Improvement As A Light Party Tio2-Nano Particle With Extract Pigment Mangostana Peel (Garcinia Mangostana) With Various Solvents". *Jurnal Bahan Alam Terbarukan.* **7** (2): 142-148. 10.15294/jbat.v7i2.14488.

[37] M. Hagos, M. Redi-Abshiro, B. S. Chandravanshi, and E. E. Yaya. (2022). "Development of Analytical Methods for Determination of beta-carotene in Pumpkin (Cucurbita maxima) Flesh, Peel, and Seed Powder Samples". *International Journal of Analytical Chemistry.* **2022**: 9363692. 10.1155/2022/9363692.

[38] H. Darmaja, H. Hardani, M. I. Darmawan, C. Cari, and A. Supriyanto. (2014). "Pembuatan Prototipe Dye Sensitized Solar Cells (DSSC) Berbasis Nanopori TiO2 Memanfaatkan Ekstraksi Antosianin Kol Merah (Brassica Oleracea Var)". *Mathematics and Sciences Forum.*

[39] R. A. Pratiwi and A. B. D. Nandiyanto. (2022). "How to Read and Interpret UV-VIS Spectrophotometric Results in Determining the Structure of Chemical Compounds". *Indonesian Journal of Educational Research and Technology.* **2** (1): 1-20. 10.17509/ijert.v2i1.35171.

[40] M. Picollo, M. Aceto, and T. Vitorino. (2019). "UV-Vis spectroscopy". *Physical Sciences Reviews.* **4** (4). 10.1515/psr-2018-0008.

[41] Z. Zurweni and A. Sanova. (2023). "Development of UV-VIS Spectrophotometer Virtual Laboratory Media for Instrumental Analytical Chemistry Digital Practicum". *Formatif: Jurnal Ilmiah Pendidikan MIPA.* **13** (1). 10.30998/formatif.v13i1.17069.

[42] S. A. Badawy, E. Abdel-Latif, and M. R. Elmorsy. (2024). "Tandem dye-sensitized solar cells achieve 12.89% efficiency using novel organic sensitizers". *Scientific Reports.* **14** (1): 26072. 10.1038/s41598-024-75959-0.

[43] T. H. Meen, C. J. Huang, S. M. Chao, J. K. Tsai, W. Water, W. R. Chen, Y. S. Liu, and L. W. Ji. (2011). "Applications of vertically oriented TiO2 micro-pillars array on the electrode of dye-sensitized solar cell". *Journal of Physics and Chemistry of Solids.* **72** (6): 653-656. 10.1016/j.jpcs.2011.02.008.

[44] W. van Bommel. (2023). In: "Encyclopedia of Color Science and Technology, ch. Chapter 126". 865-872. 10.1007/978-3-030-89862-5_126.

[45] A. Sacco. (2017). "Electrochemical impedance spectroscopy: Fundamentals and application in dye-sensitized solar cells". *Renewable and Sustainable Energy Reviews.* **79**: 814-829. 10.1016/j.rser.2017.05.159.

[46] K. Zhao, Q. Liu, L. Yao, C. Deger, J. Shen, X. Zhang, P. Shi, Y. Tian, Y. Luo, J. Xu, J. Zhou, D. Jin, S. Wang, W. Fan, S. Zhang, S. Chu, X. Wang, L. Tian, R. Liu, L. Zhang, I. Yavuz, H. F. Wang, D. Yang, R. Wang, and J. Xue. (2024). "Peri-fused polyaromatic molecular contacts for perovskite solar cells". *Nature.* **632** (8024): 301-306. 10.1038/s41586-024-07712-6.

[47] Deepak, S. Srivastava, and C. S. Malvi. (2020). "Light sources selection for solar simulators: A review". *WEENTECH Proceedings in Energy.* 28-46. 10.32438/wpe.060257.

[48] X. Ma, S. Bader, and B. Oelmann. (2017). "Characterization of Indoor Light Conditions by Light Source Classification". *IEEE Sensors Journal.* **17** (12): 3884-3891. 10.1109/jsen.2017.2699330.

[49] L. Mauri, A. Colombo, C. Dragonetti, F. Fagnani, and D. Roberto. (2022). "Iridium and Ruthenium Complexes Bearing Perylene Ligands". *Molecules.* **27** (22). 10.3390/molecules27227928.

[50] A. Sharmin, L. Salassa, E. Rosenberg, J. B. Ross, G. Abbott, L. Black, M. Terwilliger, and R. Brooks. (2013). "Photophysical studies of bioconjugated ruthenium metal-ligand complexes incorporated in phospholipid membrane bilayers". *Inorganic Chemistry.* **52** (19): 10835-45. 10.1021/ic400706u.

[51] S. Saehana, Darsikin, Muslimin, and Nasar. (2018). "Small Scale DSSC Panels Design and Its Performance". *Journal of Physics: Conference Series.* **1093**. 10.1088/1742-6596/1093/1/012034.

[52] C. G. Wu. (2022). "Ruthenium-based complex dyes for dye-sensitized solar cells". *Journal of the Chinese Chemical Society.* **69** (8): 1242-1252. 10.1002/jccs.202200225.

[53] A. Zdyb and E. Krawczak. (2021). "Organic Dyes in Dye-Sensitized Solar Cells Featuring Back Reflector". *Energies.* **14** (17). 10.3390/en14175529.